Compaction Wave Profiles in Granular HMX

Ralph Menikoff *

Theoretical Division, Los Alamos National Laboratory, Los Alamos, NM 87544

Abstract.   Meso-scale simulations of a compaction wave in a granular bed of HMX have been performed. The grains are fully resolved in order that the change in porosity across the wave front is determined by the elastic-plastic response of the grains rather than an empirical law for the porosity as a function of pressure. Numerical wave profiles of the pressure and velocity are compared with data from a gas gun experiment. The experiment used an initial porosity of 36 %, and the wave had a pressure comparable to the yield strength of the grains. The profiles are measured at the front and back of the granular bed. The transit time for the wave to travel between the gauges together with the Hugoniot jump conditions determines the porosity behind the wave front. In the simulations the porosity is determined by the yield strength and stress concentrations at the contact between grains. The value of the yield strength needed to match the experiment is discussed. Analysis of the impedance match of the wave at the back gauge indicates that the compaction wave triggers a small amount of burn, less than 1 % mass fraction, on the micro-second time scale of the experiment.

INTRODUCTION

The sensitivity of an explosive is related to material heterogeneities. When subjected to a compressive wave, the heterogeneities generate hot spots. The hot spots dominate the overall burn rate due to the strong temperature dependence of the reaction rate. In a damaged material the heterogeneities are dominated by porosity. Consequently, granular explosives are used as a model for damaged explosives.

Compression in a granular bed results in stress concentrations at the the contact between grains. When a stress concentration exceeds the yield strength, localized plastic flow occurs. The resulting change in shape of the grains enables them to pack together more tightly. Shock waves in which the compression is dominated by the decrease in porosity are known as *compaction waves*.

Hot spots resulting from a compaction wave are sub-grain in size. To better understand the formation of hot spots, meso-scale simulations — con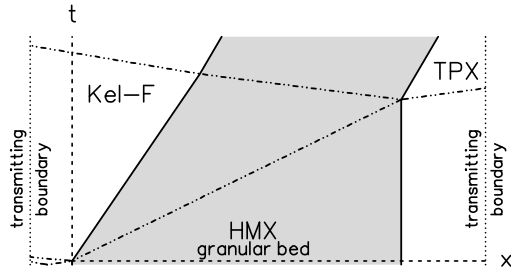tinuum mechanics calculations in which heterogeneities are resolved — are being performed. Data from experiments provide a check on the simulations.

A series of compaction wave experiments on granular explosives performed at Los Alamos and Sandia national laboratories are summarized in an article by Sheffield, Gustavsen and Anderson (4). In these experiments, a projectile from a gas gun impacts a target consisting of a front disk of Kel-F, a granular sample of HMX, and a back disk of TPX. The dominant waves in the target are shown in figure 1. Two sets of gauges are used to measure either velocity or stress. The front gauge, located at the Kel-F/HMX interface, records the wave profiles of the incident shock as it is transmitted into the granular bed, and of the return shock in the compressed bed. The back gauge, located at the HMX/TPX interface, records the wave profile as the compaction wave reflects from the back disk.

The simulations reported here correspond to experiments with a low impact velocity (280 m/s); LANL shot #912 and SANDIA shot #2477. This case is chosen in order to test that the meso-scale simulations describe quantitatively the mechanical behavior of a granular bed before proceeding to the more interesting cases of higher impact velocities

---

FIGURE 1. Wave diagram for gas gun experiments.

FIGURE 2. Initial configuration for simulations. The two light gray region at the left are Kel-F. The first region is given a velocity corresponding to the projectile. A transmitting condition at the left boundary is used to obtain the effect of a larger front disk. For the granular bed the HMX grains are shown in gray and the pores (voids) in black. The dark gray region on the right is TPX.
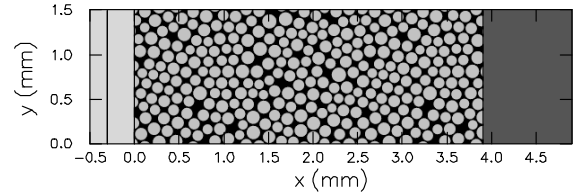
that result in significant burn on the micro-second time scale of the experiments.

Similar experiments have been simulated previously. Baer (1) used a two-phase (coarse grain) model. This type of model averages over the heterogeneities, and allows for a much coarser resolution than the grain diameter. However, an empirical compaction law is needed to account for the evolution of the porosity. In the meso-scale simulations the evolution of the porosity is determined by the plasticity model for pure HMX and the structure of the granular bed. In addition, burn models used in two-phase simulations are heuristic in nature and generally are accurate only when applied to experiments similar to the ones used to calibrate model parameters. In contrast, meso-scale simulations aim to determine the burn rate based on the measured chemical reaction rate, and the distribution of hot spots.

Horie and collaborators (5) simulated a compaction wave experiment with the discrete mesodynamics method. Though very general force laws between elements can be employed, convergence with increased resolution (number of elements per grain) and the continuum limit of the underlying model have not been studied. In addition, the focus has been on mechanical properties. Thermal quantities, such as temperature needed for reaction rates, have been neglected.

Finally, we note that 3-dimensional mesoscale simulations of reactive flow have been reported by Baer (2). Even on a super-computer, his simulation with $5\,\mu$m resolution is limited to a 1 mm cube and to a time interval of 50 ns. In order to observe reaction on this short time scale, a high impact velocity (1000 m/s) is needed. This is in the regime of a shock-to-detonation transition.

The mesoscale simulation reported here are in the

regime of a deflagration-to-detonation transition. A two-dimensional simulation with $10\,\mu$m resolution is used for a sample $3.9\,\text{mm} \times 1.5\,\text{mm}$ over a time interval of $8\,\mu$s. On the current generation of personal computers, a simulation takes well under a day.

SIMULATIONS

The initial configuration used for the meso-scale simulations is shown in figure 2. The porosity of the granular bed is 36 %. The grains are randomly distributed and have an average diameter of $120\,\mu$m with a uniform variation of ± 10 %. A Mie-Grüneisen equation of state based on a linear u_s-u_p relation is used for the Kel-F front disk and TPX back disk. An elastic-plastic constitutive model is used for the HMX grains. It consists of a Mie-Grüneisen equation of state for the hydrostatic component of the stress, an elastic shear stress, and a von Mises yield condition. The strength model is isotropic, perfectly plastic and rate independent. The material parameters are specified in (3, table 1).

Columns of Lagrangian tracer particles are placed just in front and just behind the granular bed. The column averages of the velocities and normal stresses of the tracer particles are shown along with the gauge data in figure 3. The data and simulation of the front records indicate that after a transient, the velocity and stress behind the compaction wave are in good agreement. As discussed in (3), the transient response of the tracer particles as compared to the gauges explains the initial overshoot in the simulated record. The remainder of the front records shows a slow in-
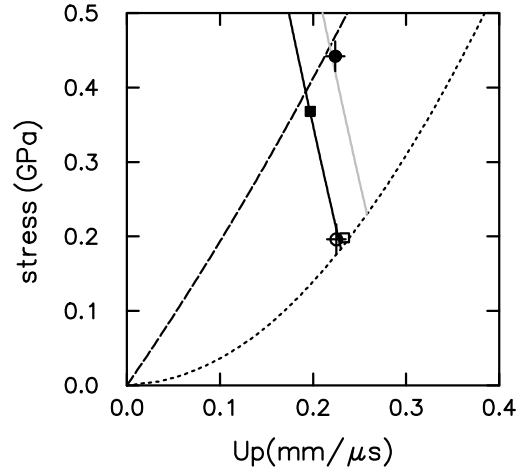
(a) Velocity gauge data, LANL Shot-912

(b) Pressure gauge data, SANDIA Shot-2477
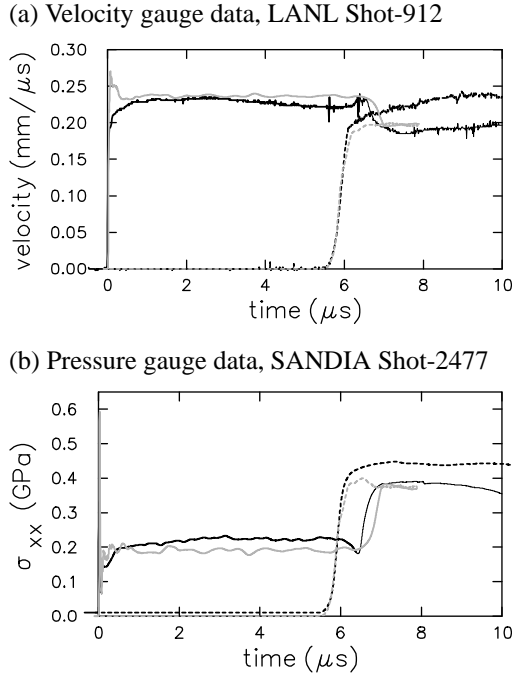
FIGURE 3. Comparison of gauge data with simulations. Black lines are gauge data taken from (4, figure 2.7). Thin line ($t > 6.4\,\mu s$) indicates possible contamination from side rarefactions. Gray lines are simulated results.

FIGURE 4. Impedance match at back gauge. Short and long dashed lines are the shock loci for the granular HMX and the TPX, respectively. Solid line is the reflected shock locus in compacted HMX. The symbols denote the states of the incident wave (from the front record) and the reflected wave (from the back record) from the experiment (squares) and simulation (circles). The crosses on the circles are an estimate of the experimental error. The gray line is the reflected shock locus assuming that burn increases the stress behind the compaction wave by 10 % as it propagates through the granular HMX.

crease of the stress and a corresponding decrease of the velocity of the gauge data as compared to the simulations. Burning behind the wave front would have this effect. In (3) it is estimated that a small amount of burn, mass fraction of less than 1 %, is sufficient to increase the stress by the observed 10 %.

At the back records, the agreement in the arrival times indicates that the compaction wave speed is correctly determined by the simulations. Using the jump condition for mass conservation, we find that the solid volume fraction ($\phi = 1 - $ porosity) behind the wave front

$$\phi = \frac{\phi_0}{1 - u_p/u_s} \, . \tag{1}$$

is nearly 1. The porosity is determined by the grain distribution and yield strength. To obtain the nearly zero porosity needed to match the wave speed, the yield strength had to be lowered to 0.15 GPa from the value of 0.26 GPa inferred from the measure elastic precursor in single crystal HMX. For comparison, we note that the average normal stress component (σ_{xx})

behind the compaction wave is 0.2 GPa. The yield strength is discussed further in (3).

The most notable discrepancies at the back records are the high values of stress and velocity at the back gauge as compared to the simulations. The difference is due to the lack of burning in the simulation. To verify this we consider the impedance match of the compaction wave impacting the back disk.

The wave curves for the impedance match are shown in figure 4. In addition, for both the experiment and the simulation the states are shown corresponding to the incident shock (as determined from the front record) and to the reflected shock (as determined from the back record). The simulation is in agreement with the impedance match.

A property of the impedance match is that the change in stress must have the opposite sign from the change in velocity. This property is violated for the data if it is assumed that the compaction wave propagates with constant strength. On the other hand, if the stress behind the compaction wave increases by

10 %, as indicated by the front gauge, then the data is consistent with the result of the impedance match.

Finally, we note that the arrival of the reflected shock at the front of the granular bed is slightly delayed in the simulation as compared to the gauge data. This is probably due to the small amount of burn occurring in the experiment and absence in the simulation.

BURNING ISSUES

The average state behind the compaction front is determined largely by the jump conditions derived from the conservation laws. The state from meso-scale simulations compares well with experimental data since it is an insensitive quantity. Because reaction rates are strongly temperature sensitive, the overall reaction rate is dominated by hot spots. Hot spots represent fluctuations, the tail of the temperature distribution, and as such are a more sensitive quantity to compute. The temperature field and the average profile are shown in figure 5. Even though the simulations do show that 'hot spots' are generated by a compaction wave, the hot-spot temperature is low and would result in a negligible amount of burn, even if reactions were included in the simulations.

Hot spots are determined by the grain distribution and dissipative mechanisms. The simulations include three dissipative mechanisms: (i) plastic work, (ii) shear heating, and (iii) artificial bulk viscosity. Conspicuously absent is frictional heating at grain interfaces. The computational problem is that algorithms that can handle the large distortion of the grains are inaccurate at interfaces and vice versa. Hence, dissipative mechanism that take place predominantly at interfaces are difficult to simulate accurately. Moreover, the peak hot-spot temperature, which is critical for reaction, requires fine resolution. Presently, on supercomputers it is possible to do simulations with sufficiently high resolution in two-dimensions but not yet in three-dimensions.

ACKNOWLEDGMENTS

The author thanks Prof. David Benson, Univ. of Calif. at San Diego, for providing the code used for

(a) Temperature field

(b) Temperature profile
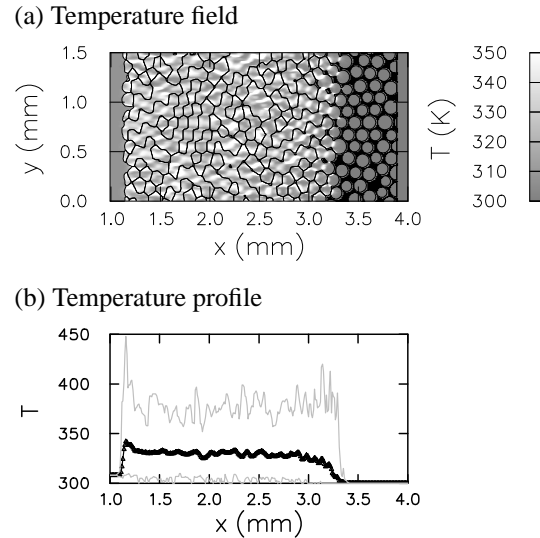
FIGURE 5. Temperature behind wave front from simulations, at time of $5\,\mu$s. Profile is average parallel to wave front (y-direction). Gray lines correspond to maximum and minimum values.

REFERENCES

1. Baer, M. R., in *High-pressure shock compression of solids IV: response of highly porous solids to shock compression*, edited by L. Davison, Y. Horie, and M. Shahinpoor, Springer-Verlag, New York, 1997 pp. 63–82.

2. Baer, M. R., in *Shock Compression in Condensed Matter–1999*, AIP, Melville, NY, 1999 pp. 27–33.

3. Menikoff, R., *J. Appl. Phys.* **(to be published)**.

4. Sheffield, S. A., Gustavsen, R. L., and Anderson, M. U., in *High-pressure shock compression of solids IV: response of highly porous solids to shock compression*, edited by L. Davison, Y. Horie, and M. Shahinpoor, Springer-Verlag, New York, 1997 pp. 23–61.

5. Tang, Z. P., Horie, Y., and Psakhie, S. G., in *High-pressure shock compression of solids IV: response of highly porous solids to shock compression*, edited by L. Davison, Y. Horie, and M. Shahinpoor, Springer-Verlag, New York, 1997 pp. 143–175.